Eur. Phys. J. D (2012) 66: 75
DOI: 10.1140/epjd/e2012-20489-6

THE EUROPEAN PHYSICAL JOURNAL D

Regular Article

Weak gravity-like force detector by "Atom interferometers"

Y. Liu[1], W.D. Li[1,a], L.B. Fu[2], and Q. Niu[1,3]

[1] Institute of Theoretical Physics and Department of Physics, Shanxi University, Taiyuan 030006, P.R. China
[2] Institute of Applied Physics and Computational Mathematics, P.O. Box 8009, Beijing 100088, P.R. China
[3] Department of Physics, The University of Texas at Austin, Austin, 78712-1081 Texas, USA

Received 22 August 2011 / Received in final form 16 December 2011
Published online 27 March 2012 –

Abstract. A weak gravity-like force detector is proposed using a novel scheme, through which the subtle modification of a weak gravity-like force on the interference pattern can be obtained. The weak gravity-like force creates two spatially imbalanced Bose-Einstein condensates (BECs) trapped in a symmetric double-well and makes a shift of the interference fringes yielded after expansion of the BECs. The strength of the weak gravity-like force is revealed by investigating the Loschmidt echo and it can be read out by analysing the density profile of interference fringes. For the weak gravity-like force, we predict that the sensitivity can be $\delta g \sim 10^{-6}$.

1 Introduction

Atom interferometry is reaching maturity as a powerful application to ultra-precise measurement [1]. As one of the most important components of atom interferometry, an "atom splitter", which generates two separated phase coherent atomic states, has been experimentally realised with the hyperfine [2] or momentum state of the atom [3]. Recently, the spatial "atom splitter" has been experimentally realised with the help of radio-frequency-induced adiabatic double-well potential on an atom chip [4–6] and other advanced optical techniques [7,8]. In analogy with an optical interferometer, the measuring quantity (usually a relative phase) can be observed with various techniques [1], depending on how the "atom splitter" works. Except for the "atom splitter", the standard interferometry schemes still require a dynamical process to accumulate the phase difference between two atomic states, and then coherently recombine them for us to read the relative phase by detecting the time-dependent population. For the spatially separated splitter, the relative phase can be observed by directly imaging the density in position space [4–7]. Although several wonderful schemes are proposed to realise Mach-Zehnder interferometer (MZI) by measuring the relative phase difference based on the physics of two weakly-linked Bose-Einstein condensates (BECs) [1,9–12], it is still interesting to search for alternative interferometric schemes which can be easily realised. In this paper, a novel scheme is proposed to realise an "atom interferometer" via interference of BECs released from a double-well. Two sets of interference fringes, the sample and reference fringes, are yielded in our scheme (Fig. 1). The sample fringes are interference fringes of BECs released from a symmetric double-well with the weak gravity-like force, while the reference fringes are ones without the weak gravity-like force. The initial states are prepared by the ground state of the symmetrical double-well with (sample) and without (reference) the weak gravity-like force. The feature of the interference actor (atoms) allows us to count the effect of the weak gravity-like force in this way: the subtle modification of the sample fringes induced by the weak gravity-like force confirmed by the Loschmidt echo [13], can be read out by simply analysing the density profile. The merit of our scheme can be found in measuring the weak gravity-like force of

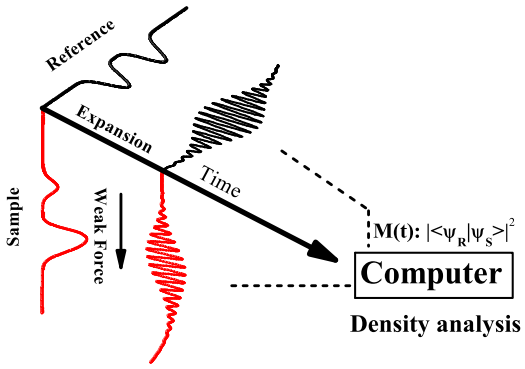

Fig. 1. (Color online) The scheme for our Atom interferometer. The Loschmidt echo ($\mathcal{M}(t)$) (or Density analysis) between the reference fringes and sample fringes are measured.

[a] e-mail: wdli@sxu.edu.cn

short-range scales (around one micrometre), and overcoming the short phase-accumulated time when considering the special interference actor (atoms) and its interatomic interaction.

2 The scheme of interferometer

As shown in Figure 1, two symmetrical double-wells are required to prepare the initial states. One is intended to prepare the initial state for the reference fringes, and the other one is set for the sample fringes titled by a weak gravity-like force. Two sets of interference fringes are yielded through the free expansions of BECs after the two symmetrical double-wells are turned off. The information on the strength of the weak gravity-like force can be extracted by density analysis in Section 4. Since the properties of the reference fringes (symmetric case) have been extensively investigated in [6,7,14,15], our focus is narrowed to the properties of sample fringes. For the sample interference fringes, the initial state, a ground state of an asymmetrical double-well, is the spatially imbalanced BECs. Here, we assume that the spatial imbalance is induced only by the gravity-like external force $(-mgz)$ along the z direction. The symmetrical double-well can be formed by combining one anisotropic harmonic potential $(\omega_x = \omega_y \equiv \omega_\perp \gg \omega_z)$ and one Gaussian-like laser beam

$$\begin{aligned} V(z) &= V_s(z) + V_g(z), \\ V_s(z) &= \frac{1}{2}z^2 + U_0 \exp\left(-\frac{z^2}{2\lambda^2}\right), \\ V_g(z) &= -\gamma z, \end{aligned} \tag{1}$$

where we have re-scaled the position space in the unit of $l_z = \sqrt{\hbar/m\omega_z}$, time in unit of $1/\omega_z$ and the energy in $\hbar\omega_z$. U_0 and λ denote the intensity and width of the laser field, respectively, while $\gamma = g\sqrt{m/\hbar\omega_z^3}$ represents the strength of the gravity-like force. In the scaled form, the one-dimension evolution of the wave function $\psi(z)$ is governed by the nonlinear Shrödinger equation or Gross-Piraevskii equation [16]

$$i\frac{\partial}{\partial t}\psi(z,t) = \left[-\frac{1}{2}\frac{\partial^2}{\partial z^2} + V_g(z) + \eta\left|\psi(z,t)\right|^2\right]\psi(z,t), \tag{2}$$

where the 1-D reduced nonlinear interaction is defined as $\eta = a_{1d}N_0/(l_z\hbar\omega_z)$, and $a_{1d} = 2a\hbar\omega_\perp$ denotes the effect of the highly transverse-confined direction (x-y direction) on the low axial direction z [17]. N_0 is the total atomic number and a is the 3-D s-wave scattering length and m is the mass of the atom. We chose the parameters of the experiment described in reference [18], where 10^5 atoms of ^{87}Rb ($a = 5.7$ nm) are trapped by an anisotropic harmonic potential ($\omega_\perp = 2\pi \times 293$ Hz , $\omega_z = 2\pi \times 24.7$ Hz). In this case, the harmonic oscillator length is $l_z = 2.170$ μm and the unit of time is 6 ms. The relation between γ and the real gravity-like constant g is $\gamma = 19.129g$. And the function of nonlinear interaction with the particle number is $\eta = 0.0612N_0$.

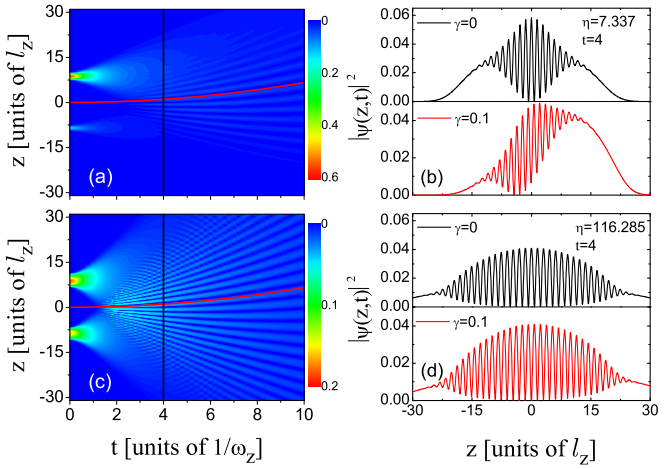

Fig. 2. (Color online) The interference pattern of imbalanced BECs for $\gamma = 0.1$. (a) $\eta = 7.337$ and (c) $\eta = 116.285$; (b) the section of (a) at $t = 4$ and (d) the section of (c) at the same time with (b). The red curve denotes the free-fall law.

Figure 2 shows how two imbalanced BECs evolve according to equation (2). The imbalanced BECs is the ground state for BECs with asymmetrical potential $V(z)$ (see Eq. (1)). The consistence in the shift of interference fringes with the free-fall law $(\gamma t^2/2)$ (red curve in Fig. 2) reveals the special characteristics of the atom. The density functions $|\psi(z,4)|^2$ for different nonlinear interactions are plotted in the right column in Figure 2. Compared with the pattern of the reference fringes (shown as black one in Fig. 2), the gravity-like force creates the asymmetrical interference pattern (see Figs. 2a–2d), while the nonlinear interaction compensates for the effect of the gravity-like force for both the initial state and the interference pattern (see Figs. 2c, 2d).

So far, we have seen that the gravity-like force works not only on the density profile of the initial states, but also on the shift of the interference fringes. Considering the short phase-accumulated time (∼12 ms) and weak gravity-like force (smaller than 0.0052 m/s^2), the major reason for this shift is the free fall of the atoms due to the external gravity-like force (see red curve in Fig. 1). This inspires us to seek a novel readout method, with which we can analyse these subtle differences between the sample and reference fringes.

3 Loschmidt echo

Loschmidt echo (LE) (or Fidelity) quantifies the sensitivity of quantum dynamics to perturbations of the Hamiltonian system. Recently, LE has been extended to the description of the dynamical properties, such as stability and phase diffusion during the dynamic evolution of BECs [13,19]. In our case, the Loschmidt echo is defined as $\mathcal{M}(t) = \left|\langle\psi_{\gamma=0}(z,t)\,|\psi_{\gamma\neq0}(z,t)\rangle\right|^2$, where $\psi_{\gamma=0}(z,t)$ and $\psi_{\gamma\neq0}(z,t)$ are the wave functions obtained by solving equation (2) for the symmetrical case ($\gamma = 0$) and the asymmetrical case ($\gamma \neq 0$), respectively. Figure 3 shows

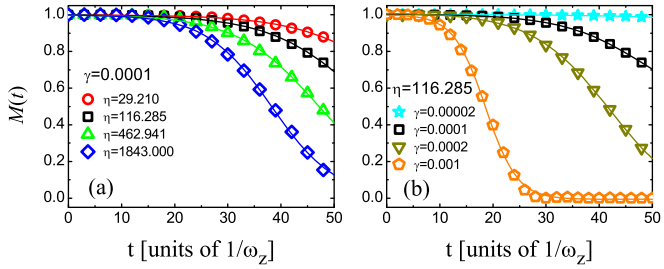

Fig. 3. (Color online) (a) The Loschmidt echo decays with time for $\gamma = 1 \times 10^{-4}$, and four different nonlinear parameters $\eta = 29.210$, $\eta = 116.285$, $\eta = 462.941$ and $\eta = 1843.000$ respectively. (b) Same as (a) but for given $\eta = 116.285$ and four different gravity constants $\gamma = 1 \times 10^{-3}$, $\gamma = 2 \times 10^{-4}$, $\gamma = 1 \times 10^{-4}$ and $\gamma = 2 \times 10^{-5}$. The solid lines are Fermi-like curves equation (3).

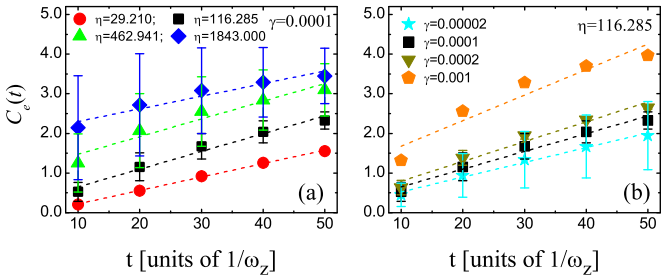

Fig. 4. (Color online) (a) The linear behaviour of the extremal contrast $\mathcal{C}_e(t)$ with time for $\gamma = 1 \times 10^{-4}$ and four different nonlinear parameters $\eta = 29.210$, $\eta = 116.285$, $\eta = 462.941$ and $\eta = 1843.000$, respectively. (b) Same as (a) but for $\eta = 116.285$ and four different gravity constants $\gamma = 1 \times 10^{-3}$, $\gamma = 2 \times 10^{-4}$, $\gamma = 1 \times 10^{-4}$ and $\gamma = 2 \times 10^{-5}$. The dashed lines are described by equation (4) and the error-bars are obtained after the $\pm 12\%$ particle fluctuation between the sample and the reference fringes is taken into account.

that the LE decays with time and this behaviour can be described by Fermi-like law [19]

$$\mathcal{M}(t) = (1 - \mathcal{M}_\infty)\left[1 + \exp\left(\frac{t - t_c}{T}\right)\right]^{-1} + \mathcal{M}_\infty, \quad (3)$$

where $\mathcal{M}_\infty$ is a small number and denotes the value of $\mathcal{M}(t)$ when the time is extended to infinity. t_c is the critical time, over which $\mathcal{M}(t)$ is going to 1/2. T determines the speed of the decay behaviour. In the symmetrical case ($\gamma = 0$), $t_c \to \infty$ and T can be a large but finite number, therefore, its LE ($\mathcal{M}(t)$) remains as one forever as the time evolution of the symmetrical wave function $|\psi_{\gamma=0}(z,t)\rangle$ is chosen as our reference. While for the asymmetrical case ($\gamma \neq 0$), t_c and T strongly depend on the nonlinear interaction and the value of the gravity-like force (γ), except that the value of $\mathcal{M}_\infty$ (0.0001) is independent of these system parameters. For the given nonlinear interaction ($\eta = 116.285$), we find that t_c exponentially deceases from 91.392 to 18.522 and T deceases from 9.824 to 2.933 when the strength of the gravity-like force is increased from 2×10^{-5} to 1×10^{-3}. Meanwhile, given the gravity-like force ($\gamma = 1 \times 10^{-4}$), similar behaviours of t_c and T are found by increasing the nonlinear interaction. This means that t_c exponentially deceases from 66.680 to 38.220 and T deceases from 9.507 to 6.108 when the nonlinear interaction is increased from 29.210 to 1843.000. The reason is that the nonlinear interaction increases the expansion velocity, and makes $\mathcal{M}(t)$ decay at a fast speed. The results show that increasing nonlinear interaction can greatly enhance the sensitivity of LE ($\mathcal{M}(t)$) to the gravity-like force (for example see Fig. 3a) where the sensitivity can be $\gamma \sim 1 \times 10^{-4}$ at $t = 50$ for $\eta = 116.285$ (see Fig. 3b). This corresponds with the release of the condensates after 0.3 second, which is still within the experimental timescale [7].

In a word, the behaviour of LE shows that there is a distinguishable difference between the sample and reference interference fringes, and that the effect of the weak gravity-like force on the interference fringes can be enhanced by increasing the strength of the nonlinear interaction. In principle, LE ($\mathcal{M}(t)$) can be measured with the help of developing quantum tomography techniques [20]. In order to avoid those difficult techniques and extract the subtle difference induced by the weak gravity-like force, one novel variable is needed. The novel variable is expected to be sensitive to both the gravity-like force and the nonlinear interaction. More importantly, it only depends on the density of the interference, which is easy to measure in the current experiments [21,22].

4 Density analysis

Based on the density of the interference, one can diagnose its characteristics with the help of visibility or contrast [23]. Considering that the space ($\mathcal{R}$) between the two light bands depends on the de Broglie wavelength of the cold atom, we take $\mathcal{R} = 0.365$, 0.364, 0.362 and 0.361, respectively, for $\eta = 29.210$, 116.285, 462.941 and 1843.000 in reference fringe. To exclude the effect of the expansion, the space has been divided by the expansion time t [15]. We then plot the average contrast $\mathcal{C}_e(t) = |\mathcal{C}_{Max}(t)| + |\mathcal{C}_{Min}(t)|$ as the function of the expansion time in Figure 4, where $\mathcal{C}_{Max,\,Min}(t)$ is the maximal or minimal value of $\mathcal{C}(z,t)$ within $\mathcal{R}$, $|\ldots|$ means taking the absolute value and the average is taken within the visibility interference range ($\mathcal{L} = 16$, 20, 30 and 40, respectively in Fig. 4a, and $\mathcal{L} = 20$ in Fig. 4b). $\mathcal{C}(z,t)$ is defined as $\mathcal{C}(z,t) = (\rho_{\gamma\neq0}(z,t) - \rho_{\gamma=0}(z,t))/(\rho_{\gamma\neq0}(z,t) + \rho_{\gamma=0}(z,t))$ and $\rho(z,t)$ is the density profile at time t. The $\pm 12\%$ density fluctuation is assumed for the shot-to-shot measurements of the sample interference and its effects (standard derivation) on $\mathcal{C}_e(t)$ are shown as error-bars in Figure 4. The linearity of $\mathcal{C}_e(t)$ with t can be approximately described as

$$\mathcal{C}_e(t) = K \times t + B. \quad (4)$$

Since the nonlinearity compensates for the effect of the gravity-like forces (see from Figs. 2 and 4a), the slope K first increases from 0.034 to 0.045, saturates around

0.045 and then decreases from 0.045 to 0.032 by increasing the nonlinear parameters from 29.210 to 1843.000 for the weak gravity-like forces ($\gamma = 1 \times 10^{-4}$). Meanwhile the value of B monotonously increases from -0.119 to 1.982. It is interesting to note that for given η, K and B are monotonously increased with the growth of the gravity-like force γ (see Fig. 4b). Since our initial states are BECs, we have ignored the phase fluctuation for each BECs, but considered the density fluctuation between the two interference sets. Figure 4 shows that the effect of the density fluctuation is proportional to the total particle number for the gravity-like force (see Fig. 4a), but this is an inverse proportional to the gravity-like force for the given total number (see Fig. 4b).

5 Further considerations

As shown in Figure 2, the weak gravity-like force creates a fraction of density distribution, which has been suggested to measure the gravity field constant with precise $\delta g/g = 2 \times 10^{-4}$ [5]. As increasing the total number of the trapped atoms compensates the fraction of density distribution induced by the gravity-like field (see Fig. 2), it will be difficult to distinguish this fraction for the weak gravity-like force. For example, the weak gravity-like force $\gamma = 10^{-4}$ induces the fraction ($\delta N/N = 0.42\%$) of density between the two wells for $\eta = 116.285$, and $\delta N/N = 0.15\%$ for $\eta = 1843.000$. In light of the real experimental conditions [18], this means we are supposed to be able to count a few (8 or 46) atoms. Owing to the particle fluctuation, this requires even more advanced techniques. In contrast, for the attractive BECs, the situation can be drastically changed. As for ^{7}Li with the same condition, even a weak gravity-like force ($\gamma \sim 7 \times 10^{-6}$) can make a huge fraction (almost 100%) of density distribution with $\eta = -0.02$. Therefore, the counting of the fractional atom distribution may be applied to measuring the weak gravity-like force with the attractive BECs (^{7}Li). For repulsive BECs (^{87}Rb), our scheme can be a better alternative. For $\gamma \sim 1 \times 10^{-4}$ (that is $\delta g \sim 5 \times 10^{-6}$), the increase of the nonlinear interaction from 116.285 to 1843.000 makes LE ($\mathcal{M}(50)$) decrease from 0.7 to 0.1, and more importantly makes the measurable $\mathcal{C}_e(t)$ increase by almost 50% (Fig. 4a) even after the $\pm 12\%$ particle fluctuation is taken into account.

6 Experimental realisation

Current experimental techniques, such as the atom chip [5,6] and optical methods [7], guarantee the realisation of the symmetrical double-well. In practice, the reference fringes can be yielded by the reference double-well, and its symmetry can be checked by flipping the double-well (means from $V(z)$ to $V(-z)$)[1] [5,24] and comparing their interference fringes at small nonlinear interaction. In this case the sample fringes can be located along the gravity-like field direction and the reference fringes will be vertical to the sample fringes. The turning-off of the double-well and the yield of the interference fringes have been done by many experimental groups [5–7]. With regard to the challenge of measuring LE [20], the density analysis method can be easily realised with the help of in situ measurement techniques, which have been experimentally applied to the study of the quantum dynamics in BECs [21,22]. Furthermore, in our scheme, the unavoidable density fluctuation between sample and reference fringes does not negatively affect the measurable variables $\mathcal{C}_e(t)$ (see Fig. 4).

[1] The fllipping of the double-well from $v(z)$ to $v(-z)$ could be experimentally realised by rotating the polarised direction of two independent orthogonal RF fields shown in [24]; or adjusting the electron currents in [5].

7 Conclusions

We have proposed a novel scheme to realise an atomic interferometry, through which the weak gravity-like force in short-range can be measured. The compensatory effect (shown in Fig. 2) and the feature of the interference actor (atoms) enables our scheme to measure the weak gravity-like force. The size ($3-80$ μm) of the experimentally realised double-well [6] ensures that the scheme works well for the short-range force. The highly developed in situ density measurement techniques [21,22] and density fluctuation investigation (Fig. 4) lead us to believe that our scheme will be realised in the near future.

This work is supported by the NSF of China (Nos. 11074155, 10674087, 10574084, 11075020), 973 program (Nos. 2012-CB921603, 2008CB317103, 2006CB921603, 2011CB921503), NCET of the Ministry of Education of China (NCET-08-0883), Graduate Innovation Project of Shanxi (No. 20093003). We gratefully thank J. Liu for the stimulating discussions.

References

1. A.D. Cronin, J. Schmiedmayer, D.E. Pritchard, Rev. Mod. Phys. **81**, 1051 (2009)
2. F. Riehle, Th. Kisters, A. Witte, J. Helmcke, Ch.J. Borde, Phys. Rev. Lett. **67**, 177 (1991)
3. A. Miffre, M. Jacquey, M. Buchner, G. Trenec, J. Vigu, Phys. Rev. A **73**, 011603(R) (2006)
4. Y. Shin, C. Sammer, G.-B. Jo, T.A. Pasquini, M. Saba, W. Ketterle, D.E. Pritchard, Phys. Rev. A **72**, 021604(R) (2005)
5. B.V. Hall, S. Whitlock, R. Anderson, P. Hannaford, A.I. Sidorov, Phys. Rev. Lett. **98**, 030402 (2007)
6. T. Schumm, S. Hoffeberth, L.M. Andersson, S. Wildermuth, S. Groth, I. Bar-Joseph, J. Schmiedmayer, P. Kruger, Nat. Phys. **1**, 57 (2005)
7. Y. Shin, M. Saba, T.A. Pasquini, W. Ketterle, D.E. Pritchard, A.E. Leanhardt, Phys. Rev. Lett. **92**, 050405 (2004)
8. L. Pezze, L.A. Collins, A. Smerzi, G.P. Berman, A.R. Bishop, Phys. Rev. A **72**, 043612 (2005)

9. J. Chwedenczuk, L. Pezze, F. Piazza, A. Smerzi, Phys. Rev. A **82**, 032104 (2010)
10. C.H. Lee, Phys. Rev. Lett. **97**, 150402 (2006)
11. G.-B. Jo, Y. Shin, S. Will, T.A. Pasquini, M. Saba, W. Ketterle, D.E. Pritchard, Phys. Rev. Lett. **98**, 030407 (2007)
12. Y.P. Huang, M.G. Moore, Phys. Rev. Lett. **100**, 250406 (2008)
13. J. Liu, W.G. Wang, C.W. Zhang, Q. Niu, B.W. Li, Phys. Rev. A **72**, 063623 (2005)
14. M.R. Andrews, C.G. Townsend, H.-J. Miesner, D.S. Durfee, D.M. Kurn, W. Ketterle, Science **275**, 637 (1997)
15. W.M. Liu, B. Wu, Q. Niu, Phys. Rev. Lett. **84**, 2294 (2000)
16. F. Dalfovo, S. Giorgini, L.P. Pitaevskii, S. Stringari, Rev. Mod. Phys. **71**, 463 (1999)
17. L. Salasnich, A. Parola, L. Reatto, Phys. Rev. A **65**, 043614 (2002)
18. C. Fort, L. Fallani, V. Guarrera, J.E. Lye, M. Modugno, D.S. Wiersma, M. Inguscio, Phys. Rev. Lett. **95**, 170410 (2005)
19. G. Manfredi, P.-A. Hervieux, Phys. Rev. Lett. **100**, 050405 (2008)
20. A.I. Lvovsky, M.G. Raymer, Rev. Mod. Phys. **81**, 310 (2009)
21. M. Albiez, R. Gati, J. Folling, S. Hunsmann, M. Cristiani, M.S. Oberthaler, Phys. Rev. Lett. **95**, 010402 (2005)
22. N. Gemelke, X. Zhang, C. Hung, C. Chin, Nature **460**, 995 (2009)
23. M. Born, E. Wolf, *Principles of Optics*, 7th edn. (expended) (Cambridge University Press, 1999)
24. T. Schumm, P. Kruger, S. Hofferberth, I. Lesanovsky, S. Wildermuth, S. Groth, I. Bar-Joseph, L.M. Andersson, J. Schmiedmayer, Quantum Inf. Process. **5**, 6 (2006)